Semi-Annual Report for January-June, 2000

Kendall L. Carder, University of South Florida

NAS5-31716

Abstract

The activities of the first half of 2000 were concentrated on quality assurance (Q/A) for our products from the new MODIS data stream. One peer-reviewed publication has been submitted for publication, and two papers are in press. A number of presentations and symposium papers were presented.

Tasks Accomplished Since January 1, 2000

1. Field experiments

a. Ecology of Harmful Algal Blooms (ECOHAB) cruises- January 10-14, and March 1-7, 2000.

Jennifer Patch, Dan Otis, Jim Ivey collected remote-sensing reflectance and water samples for absorption during an ECOHAB Gulf of Mexico and West Florida shelf experiment. The data will be used to test and adapt the global chlorophyll and CDOM algorithms for presence of bottom-reflected radiance in SeaWiFS and MODIS data.

b. Tongue of the Ocean 3 – April 23 – April 30, 2000

Robert Steward, Jennifer Cannizzaro, Daniel Otis, and Irene Antonenko collected remote sensing reflectance and water samples for absorption during a TOTO2 experiment. The data were submitted to Simbios project and were used to calibrate SeaWiFS data to evaluate effects of stray light from the adjacent shallow banks on data and algorithms.

c. COBOP99 - May 13– June 2, 2000

In conjunction with Navy-sponsored COBOP Project, a two-week exercise was conducted on the Lee Stocking Island of the Bahamas. A state-of-the-art data set was collected of inherent and apparent optical properties by investigators from various institutions. Dan Otis collected reflectance and water samples for absorption for USF. The PHILLS was flown on several transects over the area with vicarious calibration measurements conducted by USF from the R/V Suncoaster. Aerosol optical thickness (AOT) at 10 channels was measured with an automated solar radiometer along with downwelling irradiance and meteorological parameters.

USF also supported the experiment with several daily sampling trips on the RV Subchaser including remote-sensing reflectance, diffuse attenuation profiles, bottom albedo, depth, and bottom imagery. The USF slow-drop package was deployed. Remote sensing reflectance and water samples were collected for absorption

measurements. Several methods to characterize the PHILLS sensor were employed. These data will be used to modify MODIS algorithms for use in shallow waters.

2. Presentations & Symposiums

a. Initial MODIS evaluation Paper discussing data from MODIS granule 2000.2105: Carder contribution expected to fall after the Gordon contribution

While there is evidence of striping due to fixed-pattern noise in all MODIS bands of normalized water-leaving radiance $nL_w(\lambda)$, the greatest effects at visible wavelengths appear in Band 8 (412 nm). These can be brought out rather clearly by averaging pixels longitudinally(rows) and then displaying them latitudinally (columns) for each of the two boxes shown in Figure X. For color correction, we convert the data to remote-sensing reflectance values by dividing $nL_w(\lambda)$ values by $F_o(\lambda)$, the top-of-atmosphere solar radiance diffusely attenuated to the sea surface.

Figure XI displays the latitudinal variation of the data for a northern, equatorial box (a) and a southern, central-gyre box (b). Both locations manifest a significant fixed-pattern noise underlying the actual water-leaving radiance values. The perturbations are due to residual differences in the responses of each of the 10 detectors per band (lack of flat-fielding) and reflectance differences between the two mirror sides (A and B) used on alternating scans. The fixed-pattern noise repeats itself in a 10-pixel period due to detector variation per band and in a 20-pixel period due to mirror effects. Striping effects in Band 8 (412 nm), for example, are as large as 15% of the water-leaving radiance signal.

Clearly the striping is repeatable and thus removable, a task that is underway. To evaluate the utility of the present DAAC data, however, we compare its behavior to that expected for tropical, oligotrophic waters of the world ocean. After flat-fielding (e.g. normalizing to one of the 20 pixels before calibration) the data are expected to look similar to results obtained for box data that have been latitudinally averaged. These turn out to be flat, smooth lines, so they aren't displayed. The averaging will, however, reduce the random as well as the fixed-pattern noise. So actual data after flat-fielding will not be as smooth as latitudinally averaged data.

Since MODIS chlorophyll and absorption algorithms are based on models using spectral ratios of the channels, we present the behavior of appropriate ratios. In Fig. XII, we display data from the two boxes using the ratios of water-leaving reflectances from bands 8 and 9 ($r_{8,9}$) versus those of bands 9 and 12 ($r_{9,12}$). Also shown is a line ($r_{8,9}=0.95*r_{9,12}^{0.16}$) that separates tropical-subtropical field data (above the line) from

upwelling data (below the line) for relatively clear waters (e.g. where $r_{9,12} > 2.5$; Carder et al. 1999). We expect the tropical data in the boxes to fall on or above the line as they appear to do. Note that data from the clear waters of the southern box are above the line, while the average value of the more-productive waters near the equator will fall on the line. These northern points appear bi-modal, with points from the A and B sides of the mirror falling on opposite sides of the line. Flat-fielding is expected to remove the bi-modality and place these values very close to the line. Increases in colored dissolved organic matter (CDOM or gelbstoffs) reduce the $r_{8,9}$ ratio more than the $r_{9,12}$ ratio, suggesting that the CDOM in the northern box may be greater than in the southern one.

While the spectral ratios fall in the expected range, we note in Fig. XI, however, that $R_{rs}(551)$ values are perhaps 60% higher than clear-water values should be ($R_{rs}(551) = 0.0015$/sr, Gordon and Clark 1981). This indicates that perhaps an incorrect factor in the code has been applied to each band. If we multiply these values by 0.55, the radiance transmittance factor across the air-sea interface (e.g. Austin et al. 1974), $R_{rs}(551)$ values are about 0.0014 sr^{-1}, falling now in a range consistent with clear-water remote-sensing reflectances. While ratio-dependent chlorophyll a algorithms seem to perform reasonably well without this factor adjustment (see below), the back-scattering coefficients (e.g. Carder et al. 1999; Gordon and Morel 1983) and algorithms for suspended sediments (e.g. Stumpf and Pennock 1989), for example, will be over-estimated by about 60% without correction.

Figure XIII shows various chlorophyll retrievals using the MODIS DAAC data. Note that the figures contain a composite of data longitudinally averaged and latitudinally displayed for the first 50 pixels and latitudinally averaged and longitudinally displayed for the last 50 pixels. This allows one to observe the effects of fixed-pattern noise as well as simulated improvements in data quality as a result of flat-fielding. The Chl_a_3 algorithm uses bands 8, 9, and 12 (Carder et al. 1999), while the CZCS algorithm uses bands 9 and 12 (Gordon et al. 1983). The Chl_a_3d (default algorithm for Chl_a_3 (Carder et al. 1999) and OC-2 (O'Reilly et al. 1998) algorithms both use bands 10 and 12. The latter two algorithms were tuned against a global data set, however, so they are less accurate for a tropical-subtropical region. The Chl_a_3 algorithm is self-adjusting via sea-surface temperature for different bio-optical regimes, while the CZCS algorithm was validated in the subtropical regions in and near the Sargasso Sea and Gulf Stream. The differences of OC2 relative to the Chl_3_a and CZCS retrievals reflect algorithmic differences more than effects of using different band sets.

Historical data suggest that the clearest waters in the oceans are in the central gyres in the summer to early fall time frame, with chlorophyll *a* values generally in the 0.04 to 0.08 mg m^{-3} range. Chlorophyll *a* values derived using bands 8, 9, 10, and 12 for the southern box all fall within this range. Only the OC-2 data fall outside the acceptable range. This algorithm has been recently modified to an OC-3 version and adopted by the SeaWiFS Project to improve chlorophyll retrievals in the central gyre regions of the oceans.

Chlorophyll *a* concentrations retrieved for the northern box near the equatorial up-welling region of the Pacific Ocean are considerably higher than for the central-gyre box. Note that the order of algorithm retrievals has changed as well. The CZCS algorithm no longer retrieves the lowest chlorophyll concentrations. This may reflect its greater sensitivity to absorption due to colored dissolved organic matter (CDOM or gelbstoff) than the Chl_a_3 algorithm, which was specifically designed to separate gelbstoff and pigments absorption effects.

Figure XIV shows the variation of the absorption coefficient for gelbstoff at 400 nm, $a_g(400)$, for both longitudinally averaged data (pixels 0:50) and latitudinally averaged data (pixels 51:100). The fixed-pattern effects inferred by the left side of this figure will be very large without flat-fielding. Note that the fixed-pattern effects for the southern box appear smaller due to the brighter 412 nm signal there and the effect of the algorithm ratio on the pattern noise. The northern, equatorial region has twice the gelbstoff absorption found in the southern central gyre, likely accounting for the change in order of chlorophyll retrievals using the CZCS compared with the Chl_a_3 algorithms. The effects of fixed-pattern noise and sensor calibration errors will almost surely have the greatest effects on $a_g(400)$ retrievals for gelbstoff-rich waters. The CZCS, Chl_a_3d and OC2 chlorophyll algorithms all are sensitive to the increase in gelbstoff absorption found in the northern box, so the order among them for retrieved chlorophyll values remains the same for the two boxes.

After flat-fielding and correction (see above) the point clusters for the spectral ratios of Figure XII are vertically compressed in Figure XVa due to a reduction of the fixed-pattern noise in bands 8 and 9, but they are horizontally stretched due noise introduced in bands 9 and 12 through the new atmospheric-correction scheme using 3X3 averaging for the epsilon-selection process. It is thought that contamination by micro-clouds is spread by the data averaging, affecting especially the band 12 data. The ratios are presented in Figure XVb after 3X3 median filtering to remove spikes likely caused by cloud effects. While this removed most of the horizontal spreading of the data cluster, a 5X5 median average removed all of it. This suggests that perhaps the use of a 3X3 median filter in the epsilon-selection process will better eliminate contamination of the atmospheric-correction process by micro-clouds than does a 3X3 average and that perhaps the region of filtration needs to be extended to a 5X5 box around the point of correction.

A final point to be made is that although the correction process reduced the $R_{rs}(551)$ values for the central gyre region from about 0.0022 to 0.0019 sr^{-1}, it still remains 20-25% higher than is appropriate for such clear water. This is a point to be taken up during vicarious re-calibration steps for MODIS. The chlorophyll retrieval values for the algorithms all were reduced by about 30%, with the CZCS value of 0.038 mg m^{-3} bordering on the low side. If vicarious re-calibration results in lower $R_{rs}(551)$ values consistent with clear waters, it is incumbent upon the team to insure that $R_{rs}(\lambda)$ values drop according as well in order that chlorophyll *a* retrievals remain realistic.

References Cited

Carder, K.L., F.R. Chen, Z.P. Lee, and S.K. Hawes, 1999. Semianalytic Moderate-Resolution Imaging Spectrometer algorithms for chlorophyll *a* and absorption with bio-optical domains based on nitrate-depletion temperatures, *J. Geophys. Res. 104(C3)*:5403-5421.

Gordon, H.R. and D.K. Clark, 1981. Clear water radiances for atmospheric correction of coastal zone color scanner imagery, *Applied Opt. 20(24)*: 4175-4180.

Gordon, H.R. and A. Morel, 1983. *Remote Assessment of Ocean Color for Remote Interpretation of Satellite Visible Imagery: A Review*, Springer-Verlag, New York.

Gordon, H.R., D.K. Clark, J.W. Brtown, O.B. Brown, R.H. Evans, and W.W. Broenkow, 1983. Phytoplankton pigment concentrations in the Middle Atlantic Bight: comparison of ship determinations and CZCS estimates, *J. Geophys. Res. 22(1)*: 20-36.

O'Reilly, J.E., S. Moritorena, B.G. Mitchell, D.A. Siegel, K.L. Carder, S.A. Garver, M. Kahru, and C. McClain, 1998. Ocean color algorithms for SeaWiFS, *J. Geophys. Res. 103*: 24,937-24,953.

Stumpf , R.P. and J.R. Pennock, 1989. Calibration of a general optical equation for remote sensing of suspended sediments in a moderately turbid estuary, *J. Geophys. Res*. 94(C10): 14,363-14,371.

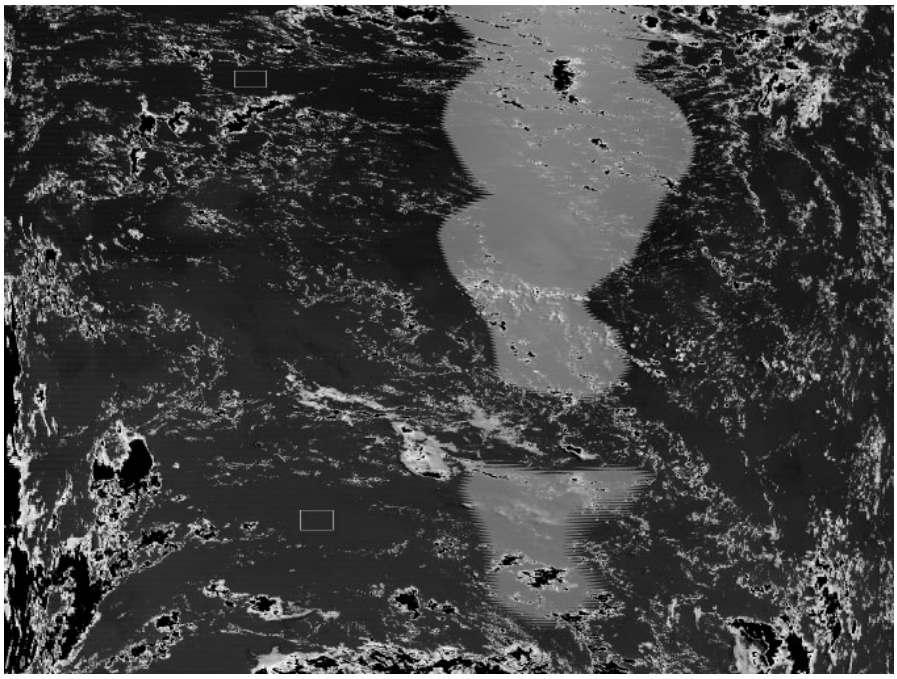

Figure X Locations of two cloud-free boxes: one contains water that is moderate in chlorophyll concentration (northern box), and the other has low concentrations. This granule is located in the south equatorial Pacific.

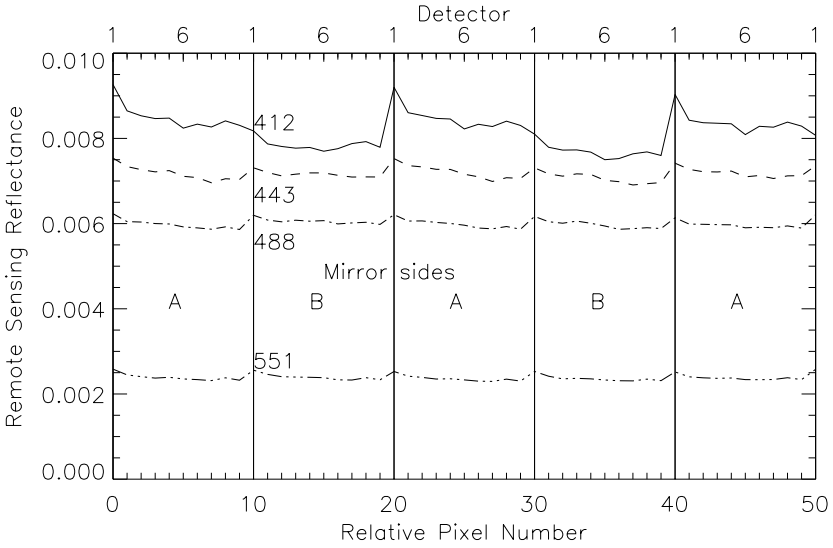

Figure XIa

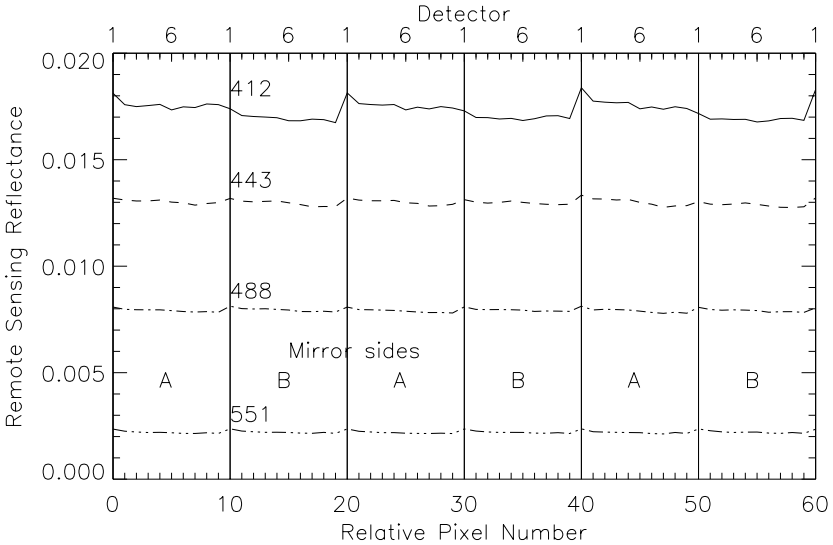

Figure XIb Latitudinal variations in remote-sensing reflectance for the northern box(a) and southern box(b). Data have been averaged longitudinally. Data shown are from detectors 1-10 for each band with an indication of which data were collected using Side A and Side B of the mirror.

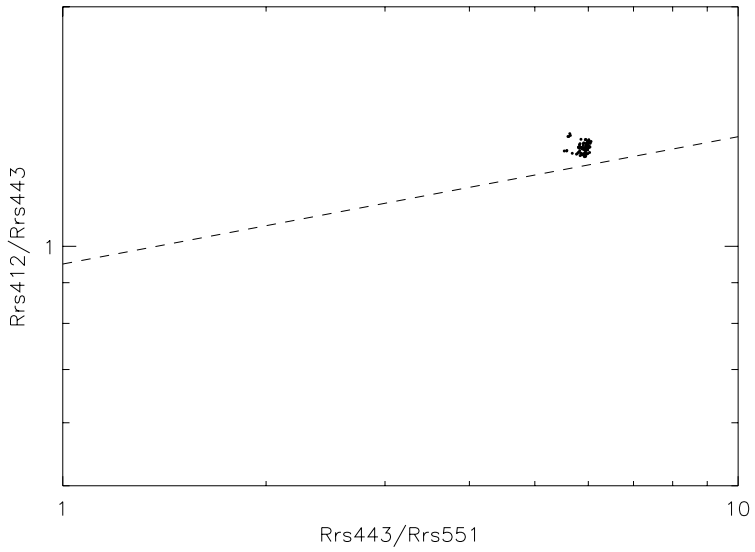

Figure XIIa

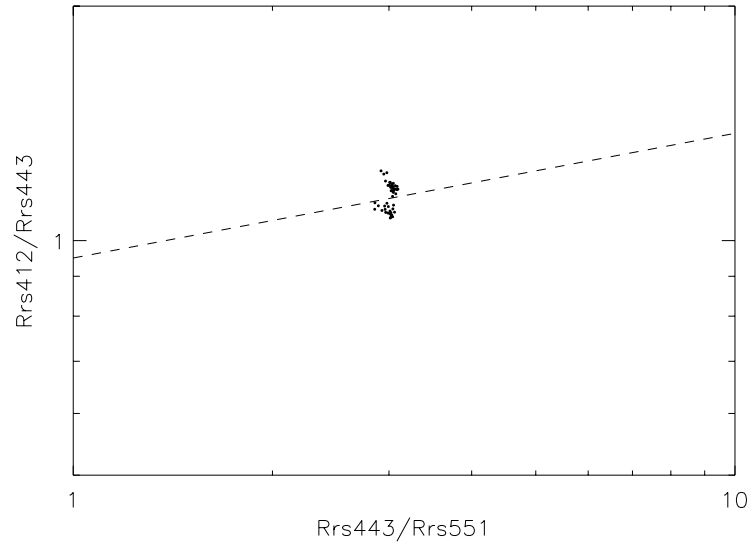

Figure XIIb Spectral ratios of remote-sensing reflectance values from the northern box(a) and southern box(b). Note that the line separates global tropical-subtropical data sets from nutrient rich ones(Carder et al. 1999).

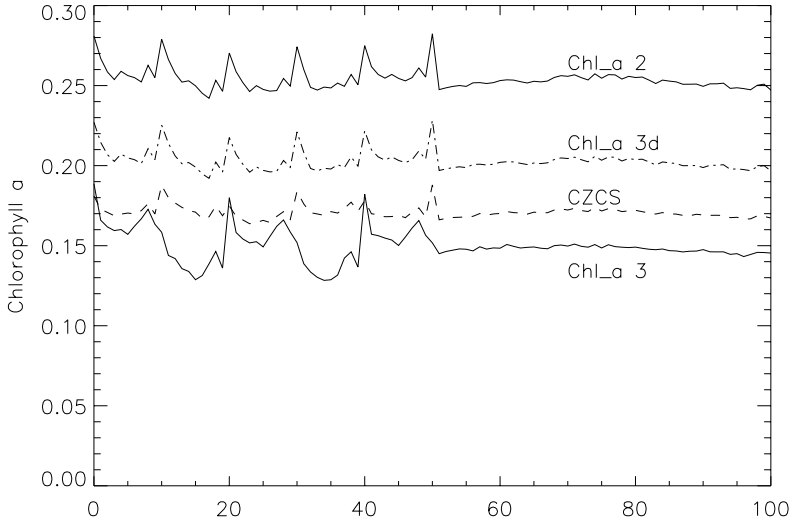

Figure XIIIa

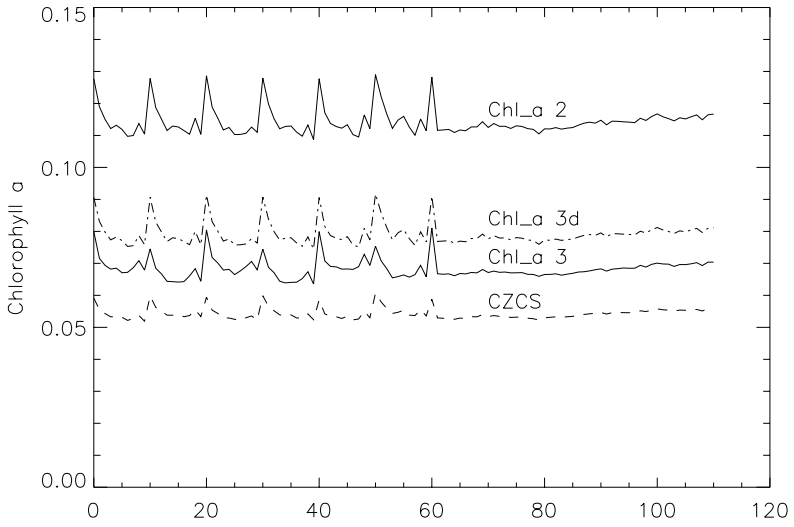

Figure XIIIb Chlorophyll retrievals using data from the northern box(a) and the southern box(b) using the CZCS algorithm(Gordon et al. 1983), the MODIS Chl a 3 algorithm(Carder et al, 1999) and the SeaWiFS OC-2 algorithm(O'Reilly et al. 1998). The first 50 pixels show latitudinal variations due mostly to striping; the last 50 pixels show longitudinal variations.

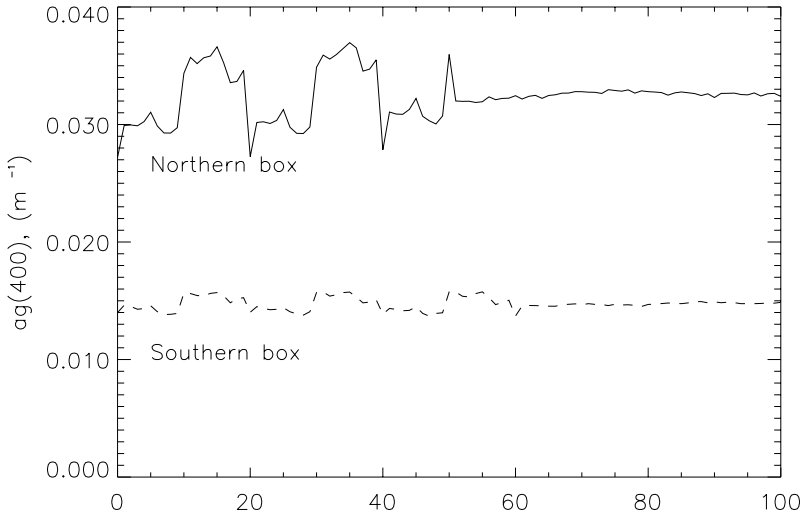

Figure XIV The absorption coefficient at 400nm due to colored dissolved organic water (gelbstoff) for the northern and southern boxes, displayed as in Fig. XIII.

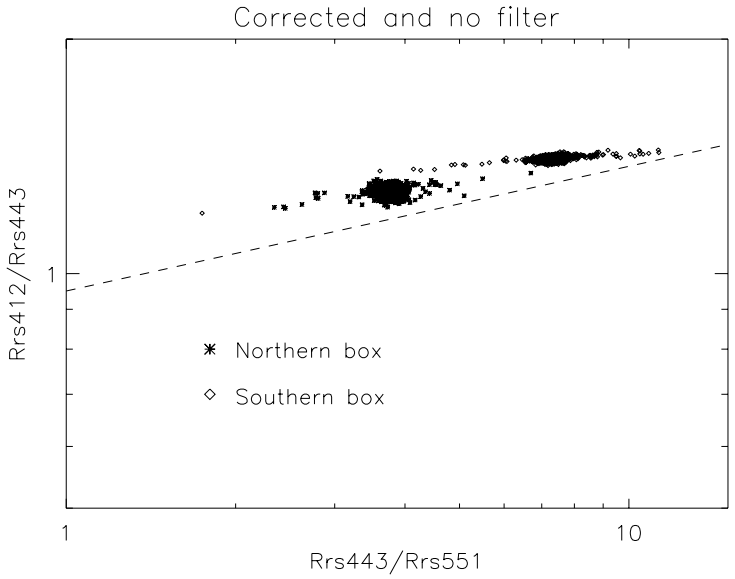

Figure XVa

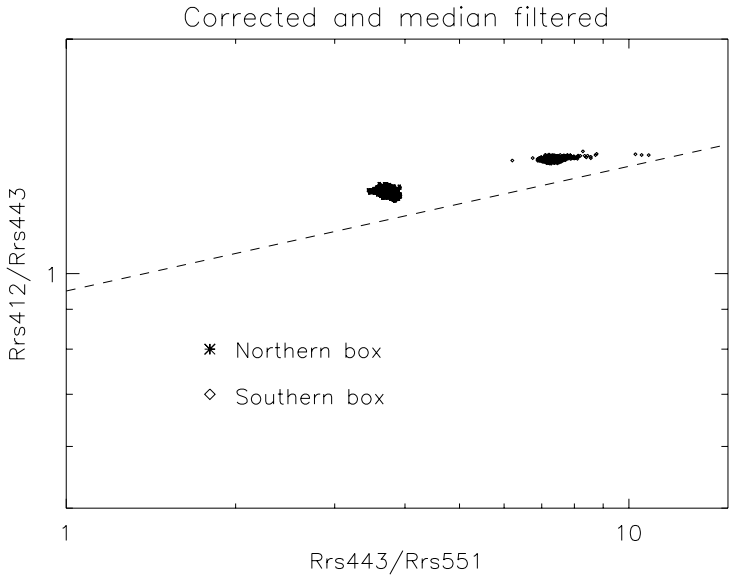

Figure XV. Spectral ratios of remote-sensing reflectance values from the northern box and southern boxes after correction: (a) results without filtering; and (b) results with 3x3 median filtering to remove micro-cloud contamination effects during epsilon selection process of the atmospheric correction step.

d. MODIS CDOM and Chlorophyll: A First Look Using SeaWiFS and AVHRR Data by Steven Hawes, Kendall Carder, F. R. Chen, and Robert Evans was submitted to SPIE's 45th Annual meeting, July 30 – August 4, 2000, San Diego, Ca., for presentation.

MODIS algorithms for the concentration of chlorophyll a and the absorption coefficients of seawater constituents such as chromophoric dissolved organic matter (CDOM) were tested using SeaWiFS and AVHRR data, and global maps of these were generated for a 2-day composite. Chlorophyll a and CDOM are important components of the global carbon budget used in estimating carbon flux from the land to the ocean and carbon uptake by primary production in the sea. The first global map of CDOM was generated, and retrieved values of chlorophyll a were consistent with field measurements from time series off Hawaii and Bermuda. This data set provided a means of testing for quality assurance in derived MODIS products using numerical filters and comparisons against ocean-climatology data sets. Of special interest was the testing of a numerical filter to flag data suspected to be in error due to effects of absorbing aerosols on the atmospheric correction. Retrieval accuracies are compared for filtered and unfiltered data, and sensitivity analyses of numerical filters are discussed.

e. Bathymetry and Environmental Properties Observed From AVIRIS Data by Z. P. Lee, Kendall Carder, and F. R. Chen was submitted to the Sixth International Conference on Remote Sensing for Marine and Coastal Environments, Charleston, South Carolina, 1-3 May 2000 for presentation.

Using a newly developed process, environmental properties of Tampa Bay were derived from recent Airborne Visible-InfraRed Imaging Spectrometer (AVIRIS) data. The derived properties include bottom depth, bottom albedo, and water absorption coefficients. The derived bottom depths were compared with bathymetry charts and found to agree very well. Also, the derived image of bottom albedo shows distinct bottom patterns, with albedo end-members consistent with sand and seagrass. The image of absorption coefficients shows the waters of the study area to be horizontally well mixed. There was no significant co-variance between water absorption and bottom properties. These results suggest that environmental properties of a large shallow-water area can be adequately obtained just from hyperspectral imaging spectrometer data. This paper allows AVIRIS to be used to quantify the depths and albedo of coastal benthic features that can affect MODIS algorithms.

f. Spectral channels and their influence on remote-sensing retrieval: 1. Shallow waters by Z. P. Lee and Kendall Carder was submitted to AGU/ASLO meeting, San Antonio, TX for presentation.

Using a newly developed remote-sensing reflectance model and optimization approach, in-water properties of shallow-water environments were derived from the remote-sensing reflectance spectrum, which covered a spectral range from 400 to 800nm. These inversions used data of every 5nm, 10nm, and 20nm, as well as MERIS, SeaWiFS and MODIS channels, respectively. This investigation is aimed at evaluating the influence of the number of spectral and spacing channels on the accuracy of remote-sensing retrievals, providing guidance

for future sensor designs. From this study, it was found for retrieving bathymetry, bottom albedo, and water absorption and scattering properties, that 1) 10nm to 20nm resolution can provide almost identical results to those using 5nm spectral resolution, 2) MERIS resolution provides very good results compared with those for 5nm, and 3) SeaWiFS or MODIS resolution can not provide accurate results regarding bottom depth, although it does provide fair accuracies for total absorption coefficients.

3. Peer-reviewed Publications

a. A paper entitled Properties of the water column and bottom derived from AVIRIS data by ZhongpingLee, Kendall. L. Carder, Robert F. Chen and Thomas G. Peacock is accepted by *J. Geophys. Res* for publication.

Using AVIRIS data as an example, we show in this study that the optical properties of the water column and bottom of a large, shallow area can be adequately retrieved using a model-driven optimization technique. The simultaneously derived properties include bottom depth, bottom albedo, and water absorption and backscattering coefficients, which in turn could be used to derive concentrations of chlorophyll, dissolved organic matter, and suspended sediments. The derived bottom depths were compared with a bathymetry chart and a boat survey and were found to agree very well. Also, the derived bottom-albedo image shows clear spatial patterns, with end members consistent with sand and seagrass. The image of absorption and backscattering coefficients indicates that the water is quite horizontally mixed. These results suggest that the model and approach used work very well for the retrieval of sub-surface properties of shallow-water environments even for rather turbid environments like Tampa Bay, Florida.

b. A paper entitled Atmospheric correction of SeaWiFS imagery: assessment of the use of alternative bands, by Hu, C., Carder, K. L., and Muller-Karger, F. E. is published on Appl. Opt. 39:3573--3581, 2000.

c. A paper entitled Atmospheric correction of SeaWiFS imagery over turbid coastal waters: a practical method by C. Hu, K. L. Carder, and F. E. Muller-Karger was accepted by Remote Sensing of the Environment for publishing.

The current SeaWiFS algorithms frequently yield negative water-leaving radiance values in turbid Case II waters primarily because the water-column reflectance interferes with the atmospheric correction based on the 765 and 865 nm spectral bands. Here we present a simple, practical method to separate the water-column reflectance from the total reflectance at 765 and 865 nm. Assuming the type of aerosol does not vary much over relatively small spatial scales (~50-100 km), we first define the aerosol type over less turbid waters. We then transfer it to the turbid area by using a “nearest neighbor” method. While the aerosol type is fixed, the concentration can vary. This way, both the aerosol reflectance and the water-column

reflectance at 765 and 865 nm may be derived. The default NASA atmospheric correction scheme is subsequently used to obtain the aerosol scattering components at shorter wavelengths. This simple method was tested under various atmospheric conditions over the Gulf of Mexico, and it proved effective in reducing the errors of both the water-leaving radiance and the chlorophyll concentration estimates. In addition, in areas where the default NASA algorithms created a mask due to atmospheric-correction failure, water-leaving radiance and chlorophyll concentrations were recovered. This method, in comparison with field data and other turbid-water algorithms, was tested for the Gulf of Maine and turbid, post-hurricane Gulf of Mexico waters. In the Gulf of Maine it provided more accurate retrievals with fewer failures of the atmospheric-correction algorithms. In the Gulf of Mexico it provided far fewer pixels with atmospheric-failure than the other methods, did not over-estimate chlorophyll as severely, and provided fewer negative water-leaving radiance values.

4. Science Meetings

MODIS Science Team, June 6-9, 2000.